JOURNAL GEOLOGICAL SOCIETY OF INDIA
Vol.79, February 2012, pp.117-134

Clay Mineralogical Studies on Bijawars of the Sonrai Basin: Palaeoenvironmental Implications and Inferences on the Uranium Mineralization

Surendra Kumar Jha[1], J. P. Shrivastava[1] and C. L. Bhairam[2]
[1]Department of Geology, University of Delhi, Delhi - 110 007
[2]Atomic Mineral Directorate for Exploration and Research, Northern Region, Delhi - 110 066
Email: jpshrivastava.du@gmail.com

Abstract: Clays associated with the Precambrian unconformity-related (*sensu lato*) uranium mineralization that occur along fractures of Rohini carbonate, Bandai sandstone and clay-organic rich black carbonaceous Gorakalan shale of the Sonrai Formation from Bijawar Group is significant. Nature and structural complexity of these clays have been studied to understand depositional mechanism and palaeoenvironmental conditions responsible for the restricted enrichment of uranium in the Sonrai basin. Clays (<2 μm fraction) separated from indurate sedimentary rocks by disaggregation, chemical treatment and centrifugation were examined using X-ray Diffraction (XRD) and Scanning Electron Microscopy (SEM). Presence of tv-1M type illite is inferred from the Rohini and Bandai Members of the Sonrai Formation, indicative of high fluid/rock interaction and super-saturation state of the fluids available in proximity with the uranium mineralization. It is observed that the Sonrai Formation is characterized by kaolinite > chlorite > illite > smectite mineral assemblages, whereas, Solda Formation contains kaolinite > illite > chlorite clays. It has been found that the former mineral assemblage resulted from the alteration process is associated with the uranium mineralization and follow progressive reaction series, indicating palaeoenvironmental (cycles of tropical humid to semi-arid/arid) changes prevailed during maturation of the Sonrai basin. The hydrothermal activity possibly associated with Kurrat volcanics is accountable for the clay mineral alterations.

Keywords: Clay mineral assemblages, Illite crystallinity, Uranium mineralization, XRD patterns, Bijawar Group, Sonrai basin.

INTRODUCTION

In Sonrai basin (Latitpur district of U.P.), uranium mineralization is associated with shale hosted bitumen, sandstone and carbonate rocks of the Sonrai Formation and chloritic shale of the Solda Formation of the Bijawar Group (Prakash et al. 1975; Singh and Bagchi, 1994; Mishra, 1996 and Roy et al., 2004). Fertile K- feldspar rich granitic basement, large number of fractures zones, high degree of illitization and Proterozoic age with unconformable sedimentary contacts represent an ideal set-up for hosting unconformity related (*sensu lato*) mineralization in this area as almost similar observations were reported by Roy et al. (2008) in the Gwalior basin. Roy et al. (2004) have reported considerable grade (0.037-0.066 % eU_3O_8 at the cut off grade of 0.01) of uranium mineralization in bituminous shale of the Rohini Member of the Sonrai Formation, suggesting different phases of mineralization that initiated high degree of remobilization. The organic matter and inorganic collides interact with each other and forms clay organic complexes. In this context the presence of organic carbon rich black carbonaceous shale and Precambrian unconformity-related uranium mineralization in Sonrai area is significant. The major clay minerals associated with sedimentary rocks are detrital in origin. They strongly reflect characters of their source material and slightly modified by their depositional environments (Weaver, 1958b, 1958c). Most of the ancient sedimentary rocks composed ~ 70% of mudstones containing ~50% clay-size fraction (Blatt et al. 1980). Clay minerals form one of the major constituents of alteration halos in the Precambrian Unconformity-Type of Uranium deposits (Hoeve and Quirt, 1987; Percival and Kodama, 1989; Iida, 1993 and Pacquet and Weber, 1993). They are significant in the understanding of hydrothermally altered halos and also provide ideas about mysterious conditions of uranium deposition. Crystal structures and crystal chemistry of clay minerals were studied (Velde, 1985;

Beaufort et al. 1992; Essene and Peacor, 1995) in the past, and these minerals have been used as indicators for the assessment of environmental conditions, including temperature, chemistry of fluids, fluid/rock ratio and redox conditions that prevailed at the time of their growth. Moreover, alterations of clay minerals offer information about uranium ions, commonly associated with clays and clay-organic complexes. They help in the understanding of the depositional mechanism and palaeoenvironmental conditions of the basin available at the time of diagenesis and hydrothermal processes. Borovec (1981) studied adsorption of uranyl species to kaolinite, illite, smectite, and chlorite particles and found that the removal of uranium by clay minerals is more effective in solution having low ionic strength.

Sonrai basin is a siliciclastic basin and possesses favourable structural features as well as hydrothermal signatures for uranium mineralization. The fractured parts of the Bandai and Gorakalan black shale is occupied by uranium-bitumen and Cu-Pb-Zn veins (Prakash et al. 1975). In this area, Bijawar hosts the uranium mineralization in the sandstones inter-bedded with a sequence of carbonate rocks (Mahadevan, 1986). Mishra (1996) stated that the uranium mineralization is in the bituminous shale of the Rohini member. Roy et al. (2004) have reported high uranium content (0.05 to 0.08% of U_3O_8) from the Bijawars of the Sonari basin and suggested three episodes of uranium mineralization (413 Ma in the bitumen, 51 Ma as fracture fill, and 1-13 Ma as U-Si complex). Uranium in bituminous shale is primarily intercepted in the boreholes rather than on the surface. The bituminous portion of the samples is pitch-black in colour, light, soft and friable, showing vitreous luster. Largely, bitumen is present in the form of fillings in the weak planes and also disseminations. The rock samples are composed of clay > fine quartz > chlorite > muscovite > sericite. Pitchblende grains associated with bitumen contain high UO_2 (90.26%) and CaO (2.34%). Dehydrogenation of organic matter due to radiation from uranium and its daughter products resulted in the high reflectivity of the bitumen, present in vicinity of pitchblende (Berger, 1974).

Proterozoic sedimentary basins not only associated with the accumulation of younger strata, but linked with the changes in the basin configuration, reactivation of various faults, hydro-geological and hydrothermal systems (Ramaekers et al. 2005a, b). Increasing paleo-weathering and hydrothermal processes were genetically related to bleaching alteration, associated with the unconformity type uranium deposit (Sopuck et al. 1983; Laverret et al. 2006). These systems have altered sedimentary and metamorphic minerals to hydrothermal clays. Chlorite and illite minerals are commonly associated with the ubiquitous secondary K-rich feldspar in the rocks located immediately above and below Precambrian-Palaeozoic unconformity (Ziegler and Longstaffe, 2000). Study on these minerals, occurring in the Sonrai area is important, offer greater insight into the nature, origin, and timing of the fluids which are responsible for the alteration of Precambrian granites and overlying rocks. Chlorite and albite form at the initial stage of alteration but, illite is considered as one of the last alteration products of K-feldspar (Harper et al. 1995). Laverret et al. (2006) have stated that the unconformity-related uranium deposits are surrounded by a host-rock alteration halos, enriched with clay minerals. Frequently, illite forms one of the main clay mineral components of the halos and displays variable crystal structures. However, mineralogical studies on clay minerals with special reference to their alteration in the Precambrian rocks of this area have not received any attention. Present work was carried out with the primary objectives aimed at the composition and structure of the clay minerals associated with the mineralized litho-units of the uranium hosted Bijawar meta-sediments to understand geochemical reasons for restricted enrichment of uranium in the clay sediments, palaeoenvironmental changes and their possible linkage with the uranium mineralization in the area. For comparison, similar but limited investigations were also carried out on the non-mineralized litho-units also.

GEOLOGICAL SET-UP

The rocks of the Bijawar-Sonrai groups were deposited in maginal basins surrounding Bundelkhand craton (Sharma, 2000), where the E-W faults represent reactivation of rift related earlier listric faults in the granitic basement, which initiated formation of Bijawar basin (Prakash et al. 1975; Srivastava, 1989). These basins occur in Sonrai, Hirapur and Gwalior areas, located south, south-east and north-west directions of the Bundelkhand Carton (Fig.1a), respectively. They preserve volcano-sedimentary units of Late Archaean to Early Proterozoic age (Sharma, 2000). The Sonrai basin (longitudes 78°45'-78°56' and latitudes 24°15' - 24°20', covers an area of 28 km length and 5-7 km width) is intra-cratonic and rectilinear in shape, trending E-W and gently dip in south direction (Fig.1b). These Palaeoproterozoic Bijawar Group (2-1.4 Ga) of rocks overlie Archaean Bundelkhand Basement Complex (3.3-2.5 Ga) and lie below rocks of the Vindhyan Supergroup (1.4-0.5 Ga). In this area, the linear Bijawar-Vindhyan sequences are unconformable, rest over pre-existing Berwar Formation. The mafic-ultramafics (meta-peridotite, meta-pyroxenite, serpentinites

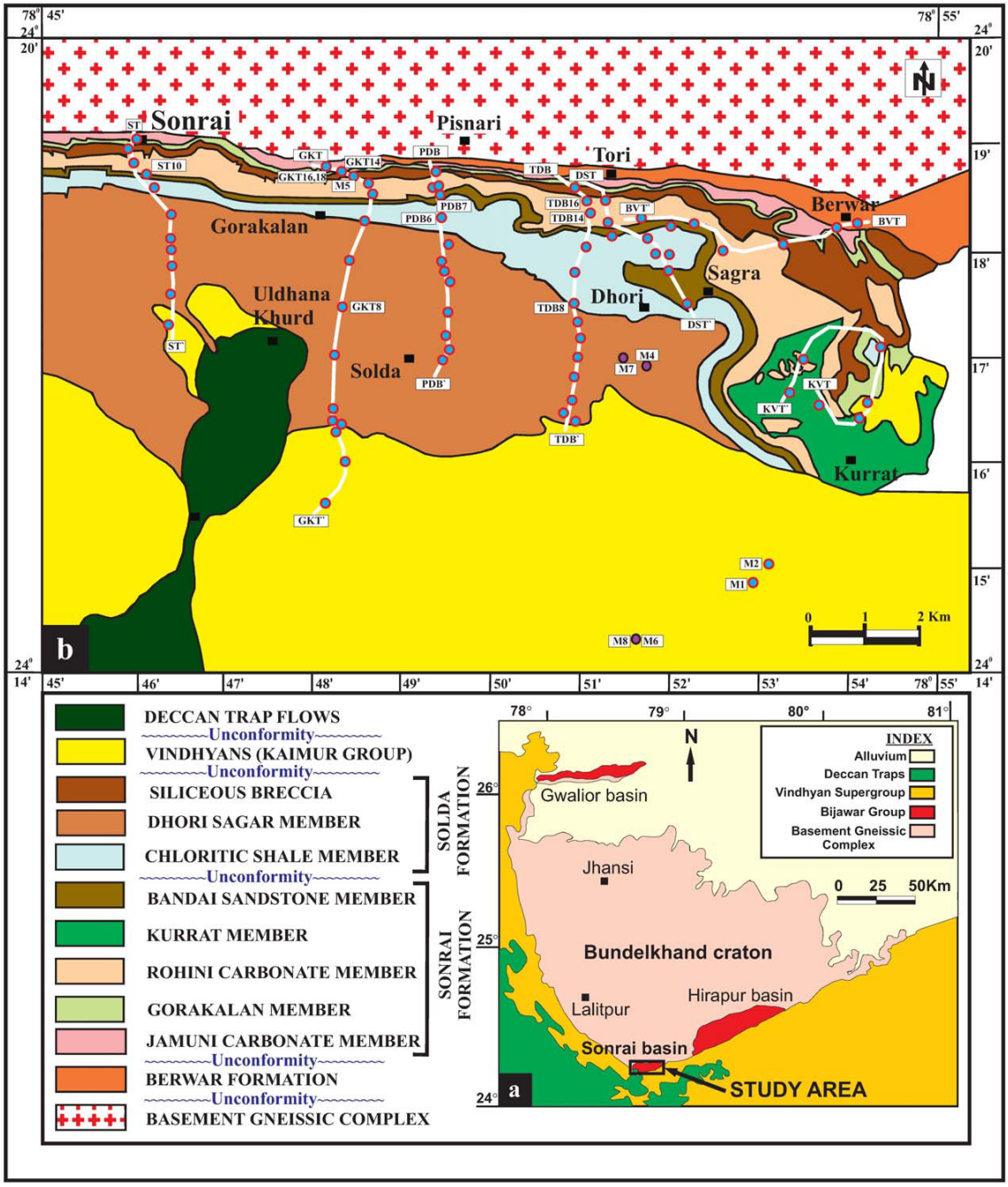

Fig.1. Map of the study area shows (**a)** Proterozoic metasedimentary (Sonrai, Hirapur and Gwalior) basins along the periphery of the Bundelkhand craton and (**b)** detailed geological map of the central part of the Sonrai basin (modified after Prakash et al. 1975).

and gabbro members) of Madaura Formation cutting across Berwar Formation and Basement Gneissic Complex (Prakash et al. 1975).

Comprehensive stratigraphic framework proposed by various workers (Singh and Goyal, 1972; Prakash et al. 1975; Srivastava, 1989; Upadhyaya et al. 1990) for Sonari area is summarized in Table 1. Singh and Goyal (1972) outlined a brief stratigraphy, but detailed stratigraphy of this area was first established by Prakash et al. (1975) who have proposed two fold sub-divisions for Bijawar rocks - Sonrai and Solda Formations and they sub-divided it into eight members. Srivastava (1989) and Upadhyaya et al. (1990) further modified the stratigraphy as proposed by Prakash et al. (1975). For the present work, the stratigraphy as proposed by Prakash et al. (1975) was considered, where the Sonrai Formations is grouped into five members such as – Jamuni

Table 1. Comparative stratigraphy of Bijawar Group of rocks in the Sonrai area, Lalitpur district, Uttar Pradesh

Singh and Goyal (1972)	Prakash et al. (1975)	Srivastava (1989)	Upadhyaya et al. (1990)	*Present work*
Basaltic Trap		Deccan Traps and dykes	Deccan Traps	*Deccan Traps*
			~~Unconformity~~~~~	*~~~~Unconformity~~~~*
Upper Vindhyan (Kaimur)	Upper Vindhyan Dulchipur, Madanpur	Vindhyan Group	Lower Vindhyan Dulachipur Mem (50mt)	*Lower Vindhyan*
~~Unconformity~~~~	~~~~~Unconformity~~~~~		~~~~~Unconformity~~~~~	*~~~~Unconformity~~~~*
	SOLDA FORMATION	SOLDA FORMATION	SOLDA FORMATION	*SOLDA FORMATION*
	Sold Member (300 m)	Solda Member	Hadda Member (1800 m)	*Solda quartzite (Ferruginous)*
	Dhorisagar Member (±20)	Dhorisagar sandstone Member	Dhorisagar Member (200-260 m)	*Dhorisagar shale & sst (Ferruginous)*
	Chloritic shale Member (±200 m)	Chloritic shale Member (200 m)	(Greenish, tuffaceous shale)	*Chloritic shale*
	~~Possible break~~~~~			*~~~~Possible break~~~~*
	SONRAI FORMATION	SONRAI FORMATION	SONRAI FORMATION	*SONRAI FORMATION*
	Kurrat Member			*(Kurrat volcanics)*
Iron Formation?	Bandai Sandstone Member (30-50 m)	Bandai Member	Bandai Member (30-50 m)	*Bandai calc. sandstone* (Interbedded shales, Pyrite)*
Upper carbonate Formation (100-200 m)	Rohini Member (±300 m) (siliceous carbonates)	Rohini carbonate Member (280-290 m) (Kurrat basic flow)	Rohini upper Member (100-125 m)	*Upper Rohini carbonates* (Filiceous, Pyrite)*
Brecciated quartzite (20-75 m)	(quartz - Jasper - carbonate breccias)		Rohini lower Member (200-225 m)	*Lower Rohini quartzite (phosphatic breccia)*
	~~Possible break~~~~~~			*~~~~Possible break~~~~~*
	Gorakalan Member (20-30 m)	Gorakalan shale Member (20-30 m)	Gorakalan Member (20-30 m)	*Gorakalan shale* (Graphitic, Siliceous)*
Lower carbonate Formation (60 m)	Jamuni Member (±180 m)	Jamuni Member (110-120 m)	Jamuni Member (180-200 m)	*Jamuni carbonates (Ferruginous, Pyrite)*
~~Unconformity~~~~~~	~~~~~Unconformity~~~~~~		~~Unconformity/ Faults~~~	*~~Unconformity/ Faults~~*
Bundelkhand granite gneisses, BHQ, basic intrusive	Basement complex (Mehroni Group)	Berwar Formation/ Bundelkhand granite complex Archaean	Bundelkhand granite and gneiss	*Archaean basement complex (Ultramafic, TTG gneisses, BIF, Amphibolite schist)*

* = *Indicates uranium mineralization in the stratigraphic units.*

carbonate, Gorakalan shale, Rohini quartzite, Rohini carbonate and Bandai sandstone. As per the presently proposed modifications in this stratigraphy, the Rohini member is divided in to Lower Rohini quartzite and Upper Rohini carbonates where, Kurrat volcanic is considered as intrusive cutting the Rohini carbonates. For better resolution and reliability of the data pertaining to spatio-temporal relationship between mineralized and non-mineralized units in the stratigraphic succession, these modifications were incorporated in Table 1. Bijawar rocks unconformably overlies the Mehroni Group (Basement complex), marked by basal conglomerate with highly weathered and eroded surface.

FIELD STUDIES

In study area, highly weathered outcrops and undulating topography (400 - 430 m. a. s. l.) with gentle slopes were observed. Seven traverses were undertaken across (N-S direction, perpendicular to the E-W strike) the basin for collection of fresh and in-situ seventy samples (each of ½ to 2 kg) from Sonrai, Solda, Madaura and Berwar Formations covered under the topographic sheet 54 L/15, (scale of 1:50,000) of Survey of India (1976). These samples were kept in the double screw capped plastic bottles to avoid contamination. Based on megascopic characters, eighteen samples were selected (representing at least 1-2 samples) from each unit of the formation for analyses (Table 2). For reconstruction of structural and geological maps of the central part of the Sonrai basin, topographic sheets and published geological maps (Prakash et al. 1975; Srivastava, 1989; Upadhyaya et al. 1990; Roy et al. 2004) have been used. The modified map divided into grids and plotted the sample locations with their respective latitude and longitude (Fig.1b).

X-RAY DIFFRACTION STUDIES

For separation of clay (< 2μm) fraction, each sample was subjected to washing, crushing, grinding, disaggregating and chemical treatment in combination of procedures as suggested by Jackson (1969), Wilson (1987) Keil et al. (1994), Yang and Apline (1997), and Tan (2005) is summarized in Fig. 2. For preparation of oriented mounts, the clay fraction is separated from the bulk sample by centrifugation and decantation methods and mounted as an oriented aggregate for clay-mineral identification. The oriented aggregate mounts force the clay mineral particles (usually plate-shaped phyllosilicates) to lie flat, allow to direct the incident X-ray beam down the Z axis of the

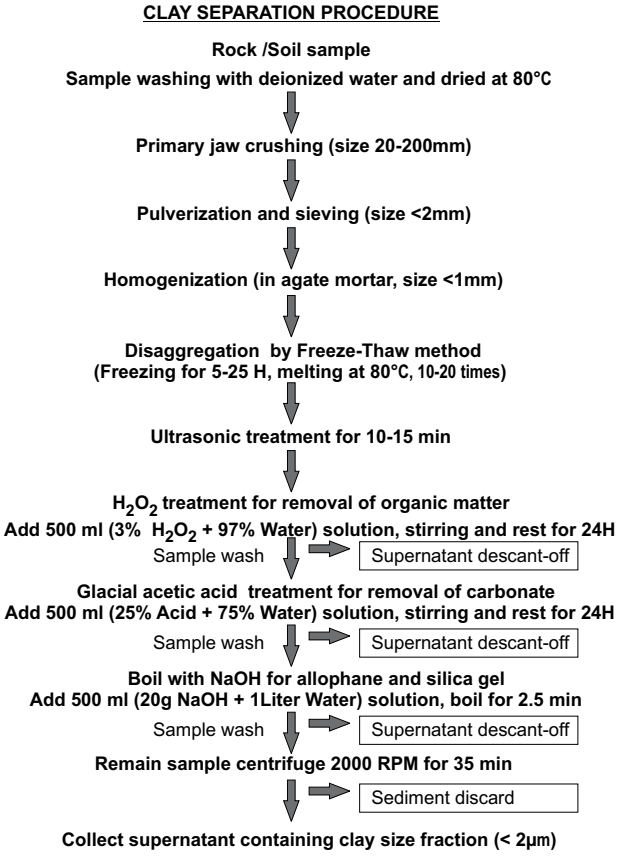

Fig.2. Chemical and mechanical procedures that were adopted for clay separation (Jackson, 1969; Wilson, 1987; Yang and Apline, 1997; Tan, 2005)

minerals and to record diagnostic basal diffractions. The Z axis shows the extent or intensity of d-spacing (expansion and contraction), indicative of certain clay minerals during subsequent treatments (Poppe et al. 2002). For this purpose, Filter-Membrane Peel Technique (Drever, 1973; Pollastro, 1982) was followed which allows a rapid and highly uniform diffraction mounts by filtering a clay suspension through the membrane filter and transferring the clay film onto a glass slide. The XRD spectra obtained by scanning, 2θ between 5 to 40° with a scanning speed of 1°/minute using Philips X Pert (Model: PW 3710) diffractometer with Cu-Kα radiations. The mineral phases were identified by comparing these spectra with standard X-ray diffraction data of the clay minerals available in the JCPDS/IDD Files (Brown, 1961; Wilson, 1987; Tucker, 1988; Tan, 2005). Clay (smectite, chlorite, Illite and kaolinite) and non-clay minerals (quartz, dolomite, feldspar, pyrite, gypsum, calcite and hematite/goethite) were identified from the Bijawar metasediments in the Sonrai basin. In these samples, two types of octahedral sheets are present in the clay minerals as discussed by Madejova (2003).

Table 2. Summarized megascopic characters of different rock units of the Bijawar Group of rocks occurring in the Sonrai basin

S. No.	Samples	Formations	Rock Units	Location (Lat. / Long.)	Megascopic Characters
1	M8	LOWER VINDHYAN	Shale	N 24°14'43.3" E 78° 51'75.5"	Fine gained, thin laminated grey colour shale
2	M6		Shale	N 24°14'43.3" E 78° 51'75.5"	Fine grained, light grey colour laminated shale
3	M3		Shale	N 24°13'24.4" E 78° 52'55.9"	Dark black, fine grained and laminated massive shale
4	M2		Vindhyan basal shale	Dhasan river Lakhanjar	Reddish brown, fine grained, laminated ferruginous shale
5	M1		Vindhyan basal shale	Dhasan river Lakhanjar	Light grey, fine grained laminated shale
6	GKT8	SOLDA FORMATION	Dhorisagarshale	N 24°17'37.2" E 78° 48'20.3"	Fine grained, laminated with ferruginous shale.
7	M4		Chloritic shale	N 24°17'11.7" E 78° 51'51.8"	Grey colour, thin laminated, silty shale
8	TDB8		Chloritic shale	N 24°17'01.0" E 78°51'00.7"	Dark grey, fine gained, massive laminated shale
9	PDB6		Chloritic shale	N 24°18'34.1" E 78°49'29.0"	Dark grey, fine grained, massive laminated shale
10	M7	SONRAI FORMATION	Bandai shale	N 24°17'11.7" E 78° 51'51.8"	Dark grey, fine grain shale
11	PDB7		Bandai sandstone	N 24°18'25.0" E 78°49'31.3"	Ferrugenous dark brown, medium grained, calc-sandstone
12	TDB14		Rohini carbonate	N 24°18'27.8" E 78°51'06.3"	Dark grey, siliceous, laminated carbonate rock
13	TDB16		Dolomitic carbonate	N 24°18'35.6" E 78°51'05.5"	Light grey, laminated, sandy carbonate rock
14	ST10		Rohini carbonate	N 24°19'05.1" E 78°45'55.9"	Siliceous, arenaceous, grey colour dolomite
15	M5		Gorakalan shale	Gorakalan village	Dark black, massive, fine grained shale
16	GKT14		Gorakalan shale	N 24°18'44.0" E 78°48'19.8"	Grey, massive layered, sandy shale
17	GKT18		Graphitic shale	N 24°19'04.0" E 78°46'23.9"	Dark, siliceous, fine gained, graphitic shale
18	GKT16		Jamuni carbonate	N 24°18'56.1" E 78°47'46.9"	Fine gained, reddish grey carbonate rock with pyrite

In dioctahedral type, two-third of octahedral sites are occupied mainly by trivalent central atoms (Al^{+3} or Fe^{+3}) and in trioctahedral type, most of the octahedral sites occupied by divalent central atoms (Mg^{+2} or Fe^{+2}). Different species of dioctahedral (kaolinite, dickite) and trioctahedral (chrysotile) minerals exist. The best-known clay minerals of the 2:1 layer type are the smectite group. The *Jamuni carbonate* of the Sonrai Formation shows high abundance of calcareous material, thus entire sample was removed during chemical treatment and clay fractions cannot be separated from the sample. The *Gorakalan shale* contains 16-29% chlorite, 11-50% kaolinite, less amount of smectites and high percentage (66-86%) of quartz (Table 3). The Mg-rich chlorites were also identified yielding basal (001) reflections at 14-14.4Å with readily observed series of high order 003 reflections at 4.7-4.8 Å and 005 reflections at 2.8 Å (Fig. 3a). Changes in the intensity or position of the basal reflections have not been observed after glycolation or moderate heating. Although, in case of GKT14 and M5 specimens (Fig. 3a), there are changes in their characteristic basal peaks (14.5- 14.7 Å) after ethylene glycol treatment (Fig. 3a) which is due to the presence of intercalated smectite layers. The characteristic basal peaks (Fig. 3a) of the kaolinite show reflections at 7.1-7.2 Å (001), 3.6 Å (002) and 3.5 Å (004). All the observed peaks are sharp and symmetrical. No change in the intensity or position of the

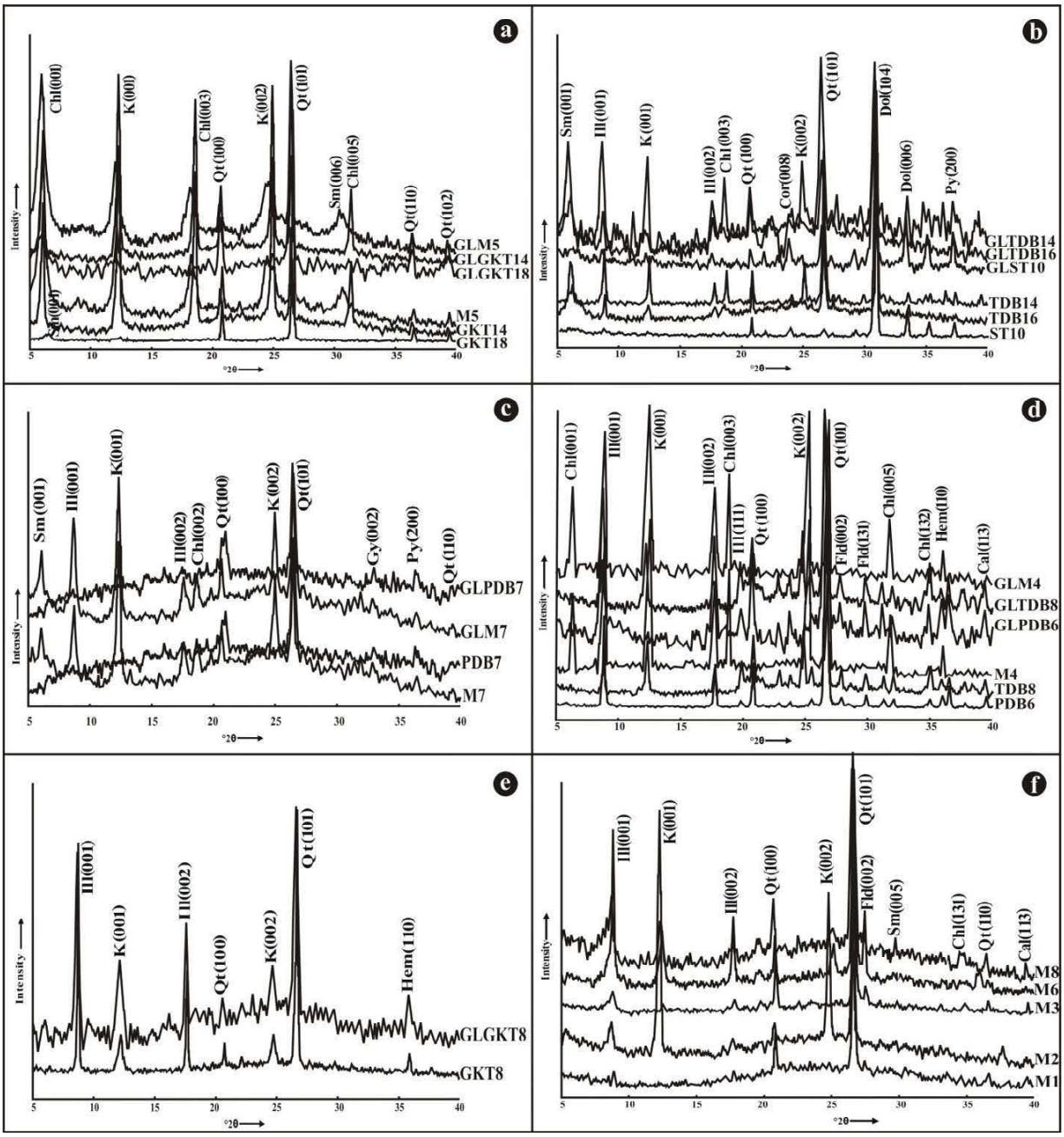

Fig.3. X-ray diffraction patterns of clay fractions obtained from **(a)** Gorakalan shales, **(b)** Rohini carbonates, **(c)** Bandai sandstone of the Sonrai Formation, **(d)** Chloritic shales, **(e)** Dhorisagar shales and (f) Lower Vindhyan shales.

basal reflections after glycolation or moderate heating is observed. Small amount of pyrite is identified at 2.39-2.4 Å. *Rohini carbonate* of the Sonrai Formation is dominated by dolomite at 2.8-2.9 Å (104), 2.67 Å (006), quartz 4.06-4.28 Å (100), 3.35 Å (101), little amount of clays (smectite, illite, chlorite and kaolinite) and less amount of pyrite (Fig. 3b). The smectite is identified by its basal (001) reflections in the region of 13.9-15 Å (Fig. 3b). When smectite is saturated with Ca and Mg-ions in the layer charges, a strong basal reflection at ~15 Å is observed (Laird, 2006). In case of montmorillonite, the expansion of two-layered structure is increased (up to 19 Å) due to the presence of water. After ethylene glycol treatment, this reflection is shifted to ~14.5-15.7 Å (Fig. 3b). Illite is abundant in the argillaceous rocks, shows strong basal (001) reflection at 10-10.3 Å in TDB14 and TDB16 specimens (Fig. 3b). The basal reflections at 10 Å are diffused and tailing towards low angle, indicating degraded nature of the mineral. Pink

Table 3. Semi-quantitative estimation of mineral phases present in the clay (0.2-2 μm) fractions obtained from Sonrai and Solda Formations

Samples	Groups	Fms.	Members	Rock units	Mineral Phases										
					Sm	Chl	Ill	K	Qt	Fld	Dol	Cal	Py	Gy	Hem
M8	LOWER VINDHYAN		MADANPUR	Light grey shale	5		9	10	75						
M6				Grey shale	2		15	8	71			5			
M3				Dark black shale		3	6	2	88						
M2				Reddish pink shale		2	2	32	60			3			
M1				Grey shale			2		96		2				
GKT8	BIJAWAR GROUP	SOLDA	DHORI SAGAR	Ferr. Shale		8	23	5	64						3
PDB6			CHLORITIC SHALE	Light grey shale		4	13		74			4			4
TDB8				Dark grey shale		9	5	13	57	5		4			7
M4				Dark shale		10	9	37	32			7			3
M7		SON RAI	BANDAI SST	Bandai shale	5	5	12	26	47				2	2	
PDB7				Bandai sandstone	6		8	7	71				8		
ST10			ROHINI CARBONATE	Grey calc carbonate	4		vw	3	7		78		5	2	
TDB16				Laminate calc carb.			3	1	25		60		vw		
TDB14				Siliceous carbonate	5	6	3	8	32		41		3		
M5			GORAKALAN SHALE	Dark black shale	6	16		11	67						
GKT14				Greenish grey shale		30		51	19						
GKT18				Graphitic shale	vw				98						

Abbreviations: Sm = Smectite, K = Kaolinite, Ill = Illite, Chl = Chlorite, Qt = Quartz, Dol = Dolomite, Cal = Calcite, Fld = Py = Pyrite, Gy = Gypsum, Hem/Goe = Hematite/Goethite and vw = Very weak peak.

siliceous carbonate (TDB14) of *Rohini Member* shows sharp peak of illite at 10 Å (Fig. 3b). The secondary (002) peak was also observed at ~5.03 Å in samples (ST10, TDB14 and TDB16). The 002 reflection is usually about one third of the intensity of the 10 Å reflections, indicating an aluminous dioctahedral nature.

The second order reflection was very weak, suggesting a trioctahedral polymorph and its presence is supported by the reflection at 1.54 Å (Fig. 3b). If the polymorph is trioctahedral, the strong third order and weak fifth order reflections suggest high Fe content (Grim et al., 1951). Illite occurring as one of the major clay phases, indicates temperature of their formation (Izquierdo et al. 1995). In the study area, the convective heat transferred from Kurrat volcanics is possibly responsible for the high proportion of hydrothermal illite at shallower depth of the basin. *Bandai sandstone* (PDB7) dominantly shows quartz (~70%) at 4.2 Å (100), 3.3 Å (101), 2.4 Å (110) reflections and weak reflections of smectite, illite, kaolinite and pyrite (Fig. 3c). Due to induration and compactness of samples, clay fractions cannot be separated in sufficient quantity. In case of sandy shale (M7), sharp peaks of clay minerals such as smectite, illite is observed. The basal reflections (001) of smectite, illite and kaolinite found at ~ 14.6 Å, 10.2 Å and 7.1 Å, respectively. Secondary reflection of kaolinite is also observed at 3.5 Å. Hydrothermal clay minerals (illite and chlorite) are used as thermo-indicators because their structure and chemical composition is sensitive to thermal changes. Temperatures based on proportion of clay minerals are in good agreement with those proposed for other

geothermal systems (Izquierdo et al., 1995). In deeply buried conditions, kaolin is most often illitized in the sandstone (Lanson et al., 2002). *Chloritic shales* of Solda Formation consist of clay minerals such as illite, kaolinite and chlorite. These samples also contain non-clay minerals including quartz, feldspar, calcite, and hematite. PDB6 is characterized by illite (001) 10.1 Å, (002) 5.04; quartz, feldspar, hematite and calcite (Fig. 3d). In TDB8 sample, clay minerals exhibit basal reflections (001) of illite at 10.2 Å and kaolinite at 7.2 Å and secondary reflections of illite (002) at 5 Å, and kaolinite (002) at 3.6 Å. The sample M4 is characterized by sharp peak of basal (001) reflections of chlorite (14.3 Å), illite (10 Å) and kaolinite (7.2 Å). No appreciable change in the diffractogram is observed after glycolation and heat treatment. Iron rich clays such as glauconite and celadonite have severely suppressed 5Å peaks. The formation of illite from a smectite precursor via intermediate mixed-layer illite-smectite (I-S) has been discussed (Hower et al., 1976; Boles and Franks, 1979). The direct precipitation of illite minerals from a kaolinitic precursor in sediments buried at shallow depths at temperatures ranging from 90 – 95°C have been discussed by Ehrenberg et al. (1993) and Lanson et al. (2002). Besides these, the stability of kaolinite with respect to illitization needs to be considered. *Dhorisagar ferruginous shale* (GKT8) consists of clay minerals (illite 23%, kaolinite 5% and chlorite 8%), quartz 64% and hematite 3% (Fig.3e). Illite is characterized by symmetric and basal reflections (001) at 10 – 10.2 Å and secondary reflections (002) as observed at 5.02 Å. Kaolinite is characterized by 7.2-7.3 Å reflections (001) and chlorite is identified at 3.6 Å (004). For comparison, Vindhyan shales were also considered, characterized by the presence of authigenic clays such as illite, kaolinite and less amount of chlorite (Fig. 3f).

The semi-quantitative analysis is used for quantification of clay minerals in the bulk samples. The peak intensity of an individual mineral is proportional to its concentration present in the sample. The intensity of diffraction patterns generally estimated either as peak height ratio or preferably peak area of a mineral in the mixture (Biscay, 1965; Tucker, 1988; Tan, 2005). Internal standard method has been used (Alexander and Klug, 1948) where quartz is used as an internal standard (Hooton and Giorgetta, 1977; Tucker, 1988). The Powder-X software is used for the measurement of relative peak height and full width at half-height (FWHM). Calculated weight percentage of mineral phases in the bulk samples is given in Table 3. Clay and non-clay mineral assemblages and their semi-quantitative analysis show distinction between Sonrai and Solda Formations. Bijawar and Vindhyan Groups also represent differences in their kaolinite + chlorite ± illite ± smectite clay contents whereas; non-clay mineral assemblage of quartz ± dolomite ± pyrite ± gypsum is associated with the Sonrai Formation (Table 4). The *Gorakalan Shale* consists of black graphitic shale (GKT18) and dark grey to black shales (GKT14 and M5), characterized by dominant presence of quartz (4.3 Å), kaolinite (7.1 Å), chlorite (14 Å) and smectite (13-15.2 Å), suggestive of dissolution of detrital quartz in response to pressure-solution mechanisms at the time of compaction of sandstones, accountable for the redistribution of silica in the secondary quartz overgrowths and consequently to rock cementation (Patrier et al. 2003). Clay mineral assemblage (K > Chl > Sm) represents large amount of authigenic kaolinite and smectite, formed by intensive weathering of rocks under high fluvial conditions in the region of humid tropical climate. The kaolinite is converted into illite and chlorite (Hower et al., 1976 and Iman and Shaw, 1985). In clay assemblage (K > Chl > Sm) from *Gorakalan graphitic shale,* the absence of illite indicates the zone of alteration, where most of the illites are converted into chlorite due to diagenetic or hydrothermal alterations. The *Rohini Carbonates* associated with siliceous carbonate (TDB14) and grey laminated calcareous carbonate (TDB16, ST10), characterized by dolomite (2.8-2.9 Å), quartz (3.3 Å), kaolinite (7.1-7.3 Å), smectite (13.9-15 Å), illite (10-10.2 Å), chlorite (4.7 Å) and pyrite (2.4 Å).

The clay assemblage (K > Sm > Ill > Chl) for Rohini carbonates indicates hydrothermal alteration in this unit, where kaolinite and smectite altered into illite and chlorite. This unit is highly altered due to paleo-weathering, tectonics and thermal activities. The *Bandai Calc-Arenaceous Sandstone* (PDB7) is inter-bedded with shale that shows combination of quartz (3.3 Å), kaolinite (7.1 Å), illite (10.2 Å), smectite (13.1-14.6 Å), chlorite (4.7 Å) and pyrite (2.7 Å). Bandai sandstone is characterized by clay mineral assemblage (K > Ill > Sm > Chl) that shows high alteration effects on illite and chlorite, atrributated to the hydrothermal conditions that prevailed during Kurrat volcanism in the Sonrai Formation. The *Chloritic Shales* characterized by quartz (3.3, 4.2 Å), kaolinite (7.1-7.2 Å), illite (10.1-10.2 Å), chlorite (14.3, 4.8 Å), calcite (2.9 Å) and goethite (2.4-2.5 Å). Light grey, fine laminated shales are characterized by the absence of kaolinite clay. Chloritic shales have a common clay mineral assemblage (K > Ill > Chl) that indicates high fluvial condition and diagenetic alteration effect on illite and chlorite. The *Dhorisagar Member* consists of ferruginous quartzite, pink ferruginous shale and sandstone (GKT8). The pink ferruginous shale is interbedded, characterized by quartz (3.3 Å), illite (10 Å and 5 Å), chlorite (3.6 Å) and kaolinite (7.2 Å). These shales

Table 4. Distinct clay mineral assemblages in the samples collected from different rock-units

Samples	Groups	Fms.	Members	Rock units	Clay Mineral Assemblages (in decreasing order)	Average Clay Mineral Assemblages (in decreasing order)
M8	LOWER VINDHYAN		MADANPUR	Light grey shale	K > Ill > Sm	K > Ill > Sm > Chl
M6				Grey shale	Ill > K > Sm	
M3				Dark black shale	Ill > Chl > K	
M2				Reddish pink shale	K > Ill > Chl	
M1				Grey shale	Ill	
GKT8	BIJAWAR GROUP	SOLDA	DHORI SAGAR	Ferr. Shale	Ill > Chl > K	Ill > Chl > K
PDB6			CHLORITIC SHALE	Light grey shale	Ill > Chl	K > Ill > Chl
TDB8				Dark grey shale	K > Chl > Ill	
M4				Dark shale	K > Chl > Ill	
M7		SON RAI	BANDAI SST	Bandai shale	K > Ill > Chl > Sm	K > Ill > Sm > Chl
PDB7				Bandai sandstone	Ill > K > Sm	
ST10			ROHINI CARBONATE	Grey calc carbonate	Sm > K > Ill	K > Sm > Ill > Chl
TDB16				Laminate calc carb.	Ill > K	
TDB14				Siliceous carbonate	K > Chl > Sm > Ill	
M5			GORAKALAN SHALE	Dark black shale	Chl > K > Sm	K > Chl > Sm
GKT14				Greenish grey shale	K > Chl	
GKT18				Graphitic shale	Sm	

Abbreviations: Sm = Smectite, K = Kaolinite, Ill = Illite and Chl = Chlorite

are characterized by a common clay mineral assemblage (Ill > Chl > K) that indicates warm arid to semi-arid climate that existed for a longer period. Illite shows diagenetic effects. The *Lower Vindhyan Shale* consists of dark black fine laminated shale (M3), pinkish shale (M2) and grey shales (M1, M6 and M8). Grey shale (M1) dominantly comprises quartz (96%) and small amount of illite (10.1 Å) and calcite (2.9 Å). Grey shale samples (M6 and M8) show similar X-ray diffraction patterns. These shales containing quartz, illite (10-10.1 Å), kaolinite (7.1 Å, 3.35 Å) and smectite (4.5-4.6 Å).The black and pink coloured shales show similar mineral assemblage of quartz (3.3 Å), illite (10.1 Å), kaolinite (7.2 Å, 3.6 Å) and chlorite (2.5 Å). These shales are characterized by a common clay minerals assemblage (K > Ill > Sm > Chl) that indicates high fluvial treatment. The kaolinite and illite data when plotted (Fig. 4) across the stratigraphic succession indicates that the cycles of tropical humid to arid/semi-arid climatic conditions were prevalent during sedimentation in the Sonrai basin.

SEM-EDS STUDIES

A high resolution scanning electron microscope (ZEISS Model - EVO50) was used to study microstructures. For this purpose, samples were coated with thin gold film to obtain maximum resolution and good quality photographs at high acceleration voltage (20 kV). The area of interest was examined in the point as well as window modes at different magnifications (10-25 KX). Clay particles acquire shape of fine plates, lamellae and tubules or elongated

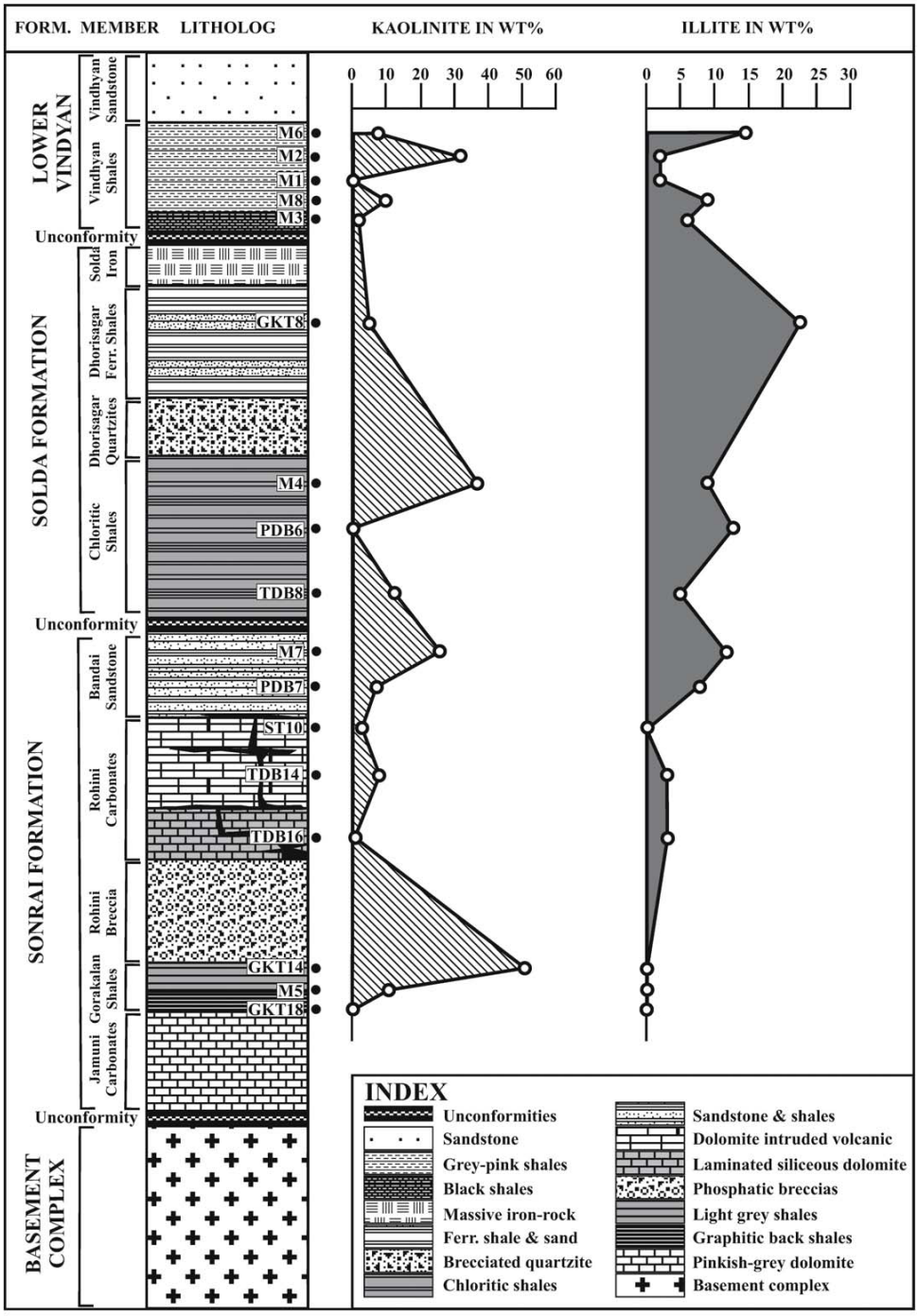

Fig.4. Clay mineralogical variation across lithostratigraphic succession of the Sonrai area, showing inverse relationship between kaolinite and illite. Kaolinite content reaches maximum (51%) in the Sonrai Formation, whereas, illite is maximum (23%) in the Solda Formation.

plates. Rohini carbonate (TDB16 and ST10) of the Sonrai Formation shows large, rectangle crystals of dolomite showing alteration into micro-aggregates (Fig. 5a and 5b). Smectite and illites show flaky and platy structures similar to that of tv-1M polytype illite that shows tube like fibrous structures. They provide porous medium or space for the clay and organic material filling along the weak zones, facilitated trapping condition for uranium ions by the process of ionic substitution and replacement. Kaolinite is found in rounded to sub-rounded form, having < 1µm size. Bandai sandstone (M7) shows large sheets of kaolinite and large flakes of smectite. On the basis of the textural and structural

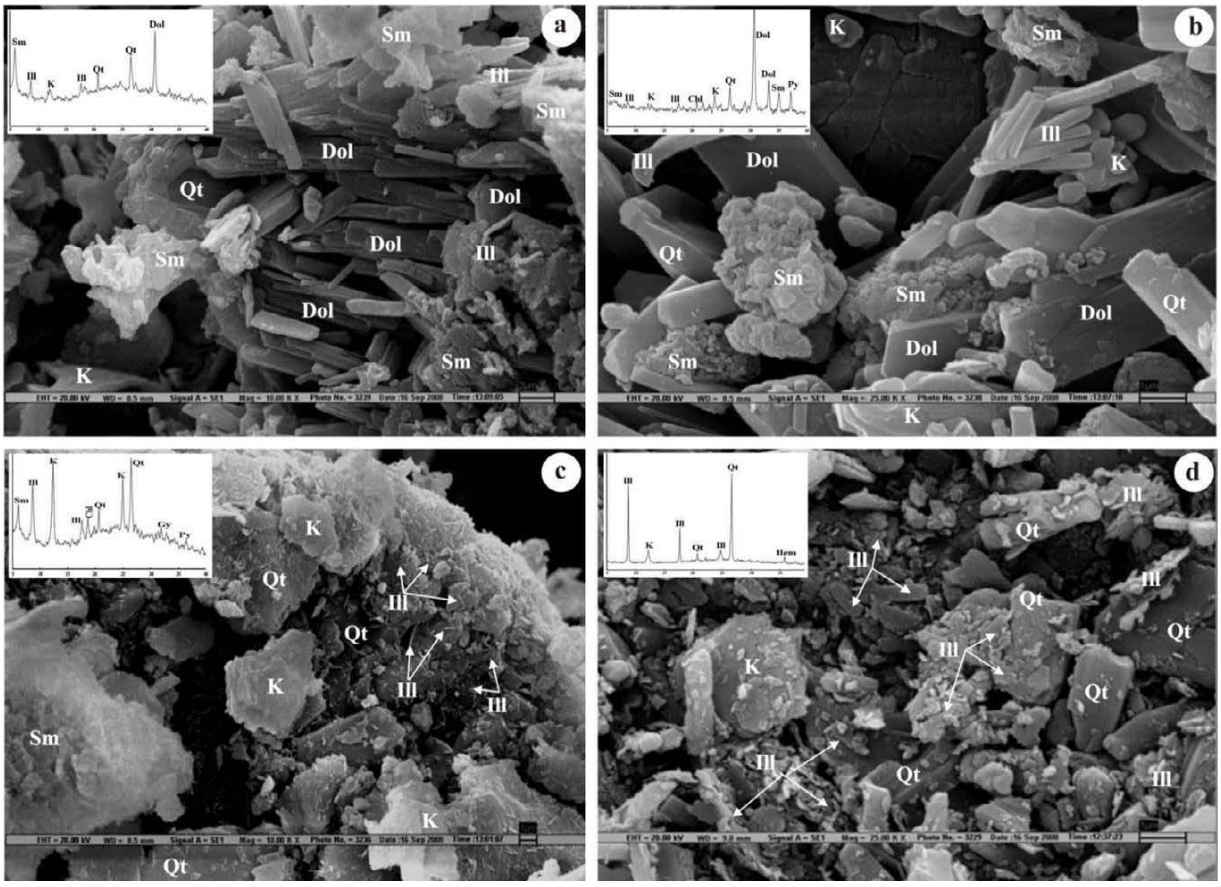

Fig.5. SEM-Back scattered electron images and XRD patterns (in the insets) with respect to clay fractions of **(a)** Rohini carbonate (TDB16) that shows crystalline dolomite and smectite, **(b)** Rohini dolomitic carbonate (ST10) shows large crystals of dolomite and tube like illite, **(c)** Bandai sandstone (M7) shows laths of smectite, kaolinite and intense population of needle or hair-like *(tv-1M polytype)* illite crystals, whereas **(d)** Chloritic shale (GKT8) shows dense micro-laths of *(cv-1M polytype)* illite.

criteria, two illite populations have been distinguished: (i) tv-1M polytype, exhibit thin (sub-micrometer) hair like shape, and (ii) cv-1M polytype (several micrometers wide), rigid lath-like illite. Fibrous illite (tv-1M type) is abundantly found in the sample (Fig. 5c). The process of illitization involves the formation of large population of illite (hydrothermally) from pre-existing kaolinite and smectite indicating uranium mineralization in this unit. Large smooth quartz crystals were also observed. Chloritic shale (TDB8) of the Solda formation showed large hexagonal shape of kaolinite and micro-laths (cv-1M polytype) of illite (Fig. 5d).

DISCUSSION

The Kurrat volcanics possibly provided hydrothermal conditions for the uranium enrichment along fractures and weak zones. The formation of clay minerals within gouges is associated with the fault activities (Hashimoto et al. 2008) where fluid-rock interaction and frictional heat controls clay composition along the fault. Uranium mineralization is accompanied by intense chloritization, hence chlorite is the main gangue mineral present in the uraniferous veins. Continental rift basins contain significant amount of neo-formed clays, commonly formed in saline or hypersaline conditions (Jones and Galan, 1988).

These conditions also have influence over the type of clays that occur in Sonrai basin, but inherited clays (illites and chlorite) normally predominate in the shields areas. A series of reactions (smectite → mixed-layer illite/smectite→ illite → muscovite) that characterize progressive increase in the illite crystallinity and decrease in the crystal defect densities; lattice strain and compositional variability as illite-muscovite becomes better ordered (Peacor, 1992). The formation of intermediate and metastable mixed-layer minerals in dioctahedral and trioctahedral 2:1 clays suggestive of the reaction progress, obeys Ostwald Step Rule (Morse and Casey, 1988; Essene and Peacor, 1995).

The reaction series (smectite→ mixed-layer chlorite/smectite →chlorite) of trioctahedral clays is observed in a wide variety of environments (Alt, 1999; Merriman and Peacor, 1999). Trioctahedral smectite is the scarce component in the Sonrai area, whereas chlorite is a common end-product of this reaction series, suggests that Fe and Mg (necessary for chlorite formation) is contributed from other reactions, most likely from dioctahedral smectite where, Fe+Mg is usually higher than that of the reaction product such as illite (Hower et al. 1976; Drief and Nieto, 2000). Although, product of the kaolin 1:1 group of minerals have been reported as minor constituents of the clay assemblages in the succession. The kaolinite transformation reaction series (kaolinite → dickite/nacrite → pyrophyllite) is well known in the sandstone (Ehrenberg et al. 1993; Ruiz Cruz and Andreo, 1996). The formation of illite or chlorite is observed in kaolinite-bearing mudstones by break down (Fe and Mg) products of kaolinite (Boles and Franks, 1979) and dickite replacement by illite in sandstone (Patrier et al. 2003). The transformation of smectite to illite is complete at this stage of evolution of the Sonrai basin, indicates effects of converting soft clays and mudstone into well-lithified, brittle mudstones and shales (e.g. Gorakalan and chloritic shales of Sonrai basin). The reaction-progress is measured using percentage of illite in the illite-smectite mixed clays, or clay "crystallinity". Three types of observations and measurements (Merriman and Peacor, 1999) have been made to evaluate reaction progress in transformed clay minerals (indicate maturity of sedimentary basin) - clay mineral assemblage, quantification of mixed-layers and clay mineral "crystallinity". Clay minerals are subjected to complexity in nature by tectonic deformations and recycling of alteration process several times in the Sonari basin. It is well established (Tucker, 1988) that illite is characterized by minimal leaching conditions as in the temperate and higher latitudes. Chlorite is also formed under this condition, where it is easily oxidized. Illite and chlorite form under arid conditions where chemical processes are limited. Smectite is produced where the degree of leaching is intermediate or poorly drained. They also form in alkaline and arid conditions. Kaolinite forms in the tropical environment, where acid leaching is intensive. There are evidences for chemical alteration of clays, such as Na, Mg and K absorbed on the clay surfaces and into their internal structure for Ca exchange. In the burial diagenetic environment, there is a progressive alteration of the clay minerals with rising temperature. One of the first transformations is the smectite to smectite-illite (mixed-layer) and then it proceeds to illite (Van de Kamp, 2008). Retallack (1986a) demonstrated that the kaolinite decreases with increasing illite and chlorite. Illite-rich illite-smectite complexes and chlorite found in this area indicate that clay matrix is still at the deep diagenetic stage.

The value of full width at half-height (FWHM) for the illite (001) reflection is referred to Kubler Index (Kubler, 1984) or the 'illite crystallinity index' which is used to measure degree of metamorphism of very low-grade, pelitic rocks (Frey and Robinson, 1999; Guggenheim et al., 2002). The width of the illite (001) peak is related to crystal-chemical factors such as domain size and swelling. X-ray diffraction data obtained from oriented clay specimens have been used. Notable increase in the degree of crystallinity indicates changes in the chemical composition of the illite in the late diagenetic to early stage of metamorphism. The grade of metamorphism increases with the rise in the ratio of the Al/Fe+Mg as calculated from the intensity ratio of the illite 5 Å and 10 Å $I_{(002)}$ / $I_{(001)}$ peaks (Dunoyer de

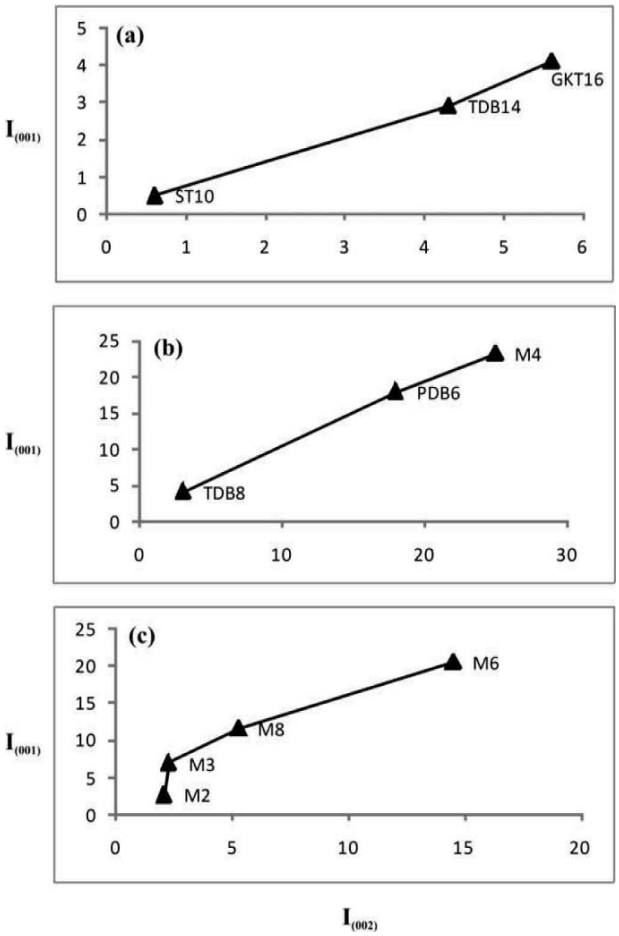

Fig.6. The trend of metamorphism increases with the increase in the ratio of Al / (Fe + Mg) that corresponds to the intensity ratios of the illite ($I_{(002)}$ / $I_{(001)}$) at 5 Å and 10 Å reflection peaks over X-ray diffractograms for (a) Rohini Carbonates of the Sonrai Formation, (b) Chloritic Shales of the Solda Formation and (c) Basal Lower Vindhyan Shales.

Table 5. Srodon Intensity Ratio (KI) for illite (100) 10Å and illite (002) 5Å values for different samples

Rock source	Bulk-rock mineral assemblages	Clay mineral assemblages	Samples	KI of 10Å illite $_{(001)}$ (Value in °2θ)		Intensity ratio of AD	KI of 5Å illite $_{(002)}$ (Value in °2θ)		Intensity ratio of EG	Srodon intensity ratio	FWHM of Illite$_{(001)}$
				AD	EG		AD	EG			
Lower Vindhyans											
Grey shales			M6	0.08	0.12	0.32	0.16	0.20	0.71	2.23	1.06
Pink ferr. Shales	(K + Ill +	(K + Ill +	M2	0.32	0.12	0.59	0.24	0.32	0.78	1.32	1.03
Grey shales	Chl + Sm+	Chl + Sm)	M1	0.96	0.96	0.91	0.96	0.94	1.00	1.10	1.04
Light grey shales	Qt + Cal +		M8	0.12	0.12	0.33	0.40	0.32	0.46	1.37	1.00
Black shales	Dol)		M3	0.16	0.60	0.14	0.48	0.64	0.40	2.96	1.06
Madanpur Formation											
Bijawar Group											
Dhorisagar ferr. Shales	(K + Ill +		GKT8	0.08	0.12	0.74	0.12	0.16	0.94	1.28	1.06
Chloritic dark shale	Chl + Qt +	(K + Ill +	M4	0.08	0.10	0.47	0.10	0.10	1.07	2.28	1.05
Light grey shales	Hem/Goe+	Chl)	PDB6	0.12	0.24	1.00	0.08	0.20	1.04	1.04	1.00
Dark grey shales	Cal ± fld)		TDB8	0.12	0.16	1.18	0.12	0.24	0.76	0.64	0.78
Solda Formation											
Bandai shales			M7	0.20	0.12	0.37	0.32	0.16	0.45	1.23	0.86
Interbedded sandstone			PDB7	0.00	0.00	0.00	0.00	0.00	0.00	0.00	0.00
Rohini grey carbonates			ST10	0.20	0.24	1.75	0.24	0.24	1.20	0.69	1.16
Siliceous carbonates	(K + Chl ±	(K + Chl ±	TDB14	0.10	0.20	0.77	0.16	0.32	0.54	0.70	1.04
Laminat grey carbonates	Ill ± Sm Qt ± Dol ±	Ill ± Sm)	TDB16	0.08	0.20	0.47	0.32	0.24	1.37	2.91	0.82
Gorakalan grey shales	Py ± Gy)		GKT14	0.00	0.00	0.00	0.00	0.00	0.00	0.00	0.00
Black shales			M5	0.00	0.00	0.00	0.00	0.00	0.00	0.00	0.00
Graphitic shales			GKT18	0.00	0.00	0.00	0.00	0.00	0.00	0.00	0.00
Sonrai Formation											

Abbreviation: AD = values from air-dried and EG = values from ethylene glycol-solvated XRD patterns. K = Kaolinite, Ill = Illite, Sm = Smectite, Chl= Chlorite, Qt = Quartz, Dol = Dolomite, Cal = Calcite, Py = Pyrite, Gy = Gypsum, Hem = Hematite and Goe = Goethite.

Segonzac, 1970). Corresponding to intensity ratio of the illite peaks, Rohini carbonates of the Sonrai Formation is characterized by low grade of metamorphism. Laminated calcareous carbonate (GKT16) shows relatively high degree of metamorphism as compared to the siliceous carbonates (TDB14, ST10) samples (Fig. 6a). Chloritic shales of the Solda Formation are characterized by relatively moderate degree of metamorphism by their corresponding $I_{(002)}$/ $I_{(001)}$ peaks intensity ratios. Grey shales (TDB8, PDB6) show relatively high grade of metamorphism (Fig. 6b) than the dark shale (M4). Dark and grey shales (M3 and M8 samples) represent (Fig. 6c) higher grade of metamorphism comparing to grey (M1, M6) and pink shales (M2). Using Srodon intensity ratio (Srodon, 1984), crystallinity of illite was determined from the air-dried and glycolated diffraction patterns. The full width of the basal reflection (I_{001}) of illite was measured (Table 5) at half-height above background level, using equation [Ir = (001/003) $_{\text{air dried}}$ / (001/003)$_{\text{glycolated}}$]. But, in the present study, the basal reflection of illite at 10 Å and 5 Å is considered as maximaum reflection peaks.

The value of Srodon intensity ratio (Ir) determined by KI values from illite $_{(001)}$ and illite $_{(002)}$ in °2θ of both air dried and ethylene glycol solvated diffraction data (Table 5). This ratio is very sensitive and varies with the presence of swelling layers in the illite. If the value of Ir > 1.0, the illite has swelled to some degree but, if Ir = 1.0, the illite has no detectable tendency to swell. Detectable range of expendability (1.04-2.96) indicates that the Sonrai samples are of highly swelling type within the combination of tetrahedral and octahedral layers due to hydration and cation exchange capability. The crystallinity index and the Srodon intensity ratio measured for illite samples plotted (Fig. 7) to determine mean X-ray scattering domain size and expandability, shows three metamorphic zones as defined on the basis of the Kubler Index (Kisch, 1983).

The crystallinity index of illite have a variety of expandabilities depending on the value of (N). It is postulated that the broadening of illite peak is due to swelling and structural distortions, attributed to the presence of coherently diffracting chlorite layers in the illite crystals (Ahn et al*.,* 1988) affecting peak width. Most of the data

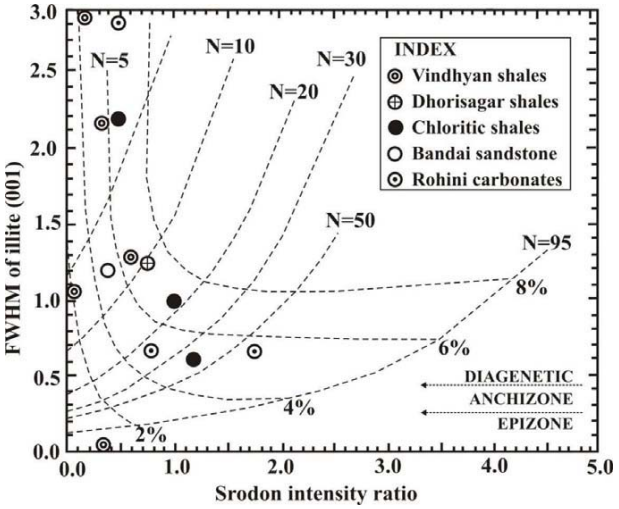

Fig. 7. Srodon intensity ratios plotted for the determination of mean XRD scattering domain size (N) and percentage of swelling layers (%) for illite using crystallinity index (FWHM) of Rohini carbonates, Bandai sandstones, Chloritic shales, Dhorisagar shales and Vindhyan shales.

plots for these samples lie within the diagenetic region (Fig. 7). Rohini carbonates are characterized by 6-8% swelling and expandability (N > 50), indicate thick layer of illite that exists in the oriented slide. Values obtained for Bandai Sandstone of the Sonrai Formation is N =10 and swelling of 6%. Chloritic shales of Solda Formation shows values in the range of N = 10 - 50 and swelling of illite layers found to be 4-6% (Fig. 7). Dhorisagar Ferruginous Shales shows values of 8% for swelling and expandability N =10. Lower Vindhyan shales are characterized by 2-6% swelling and N = 5-10 expendability. Formation of illite particles, having high values of N is favoured by pore fluids which are slightly supersaturated with respect to illite solubility. Under these conditions, illite crystals show spiral growth patterns, reflecting availability of hydrothermal systems or the area is regionally metamorphosed (Eberl and Srodon, 1988). Variation in the structural and textural properties of illite resulting from the nucleation and growth kinetics is indicative of changes in the flow regime and saturation state of the fluid during their formation. The tv-1M illite present in the Bandai Sandstone (Fig.5c) is favoured in the environment characterizing high fluid/rock ratios and super-saturation state of the fluids available in proximity with the U mineralization (Beaufort et al. 2005).

CONCLUSIONS

In the present study, an attempt is made to understand the nature of clay minerals formed due to paleo-weathering and alteration of pre-existing minerals or rocks in different climatic set-up and their spatio-temporal relationship with uranium mineralization in Sonrai basin. The presence of high amount of kaolinite and less amount of illite in the lower units of the Sonrai Formation indicates high rainfall in tropical humid climatic conditions which led to intense weathering, swift erosion and rapid sedimentation in initial stage of deposition. Increasing amount of illite and their crystallization (illitization) and decreasing kaolinite for Rohini carbonates and Bandai calc-sandstone shows slightly warm or semi-arid climatic conditions and scanty or low rainfall. The consequent effect of hydrothermal activity possibly associated with the Kurrat volcanics during reactivation of rift is accountable for high degree of illitization within Rohini and Bandai members. Thick sequence (200 m) of chloritic shales of Solda Formation contains superior kaolinite and lesser quantity of illite that indicates repetition of humid tropical climatic conditions with heavy rainfall for a longer duration. It was possibly a prominent region for the deposition of massive and thick pile of chloritic shale in the basin. The arid and warm climatic conditions prevailed during the formation of the upper sequences of the Solda Formation. Data reflect high proportion of illite whereas, kaolinite shows negative anomaly for the deposition of Dhorisagar ferruginous shale inter-bedded with sandstone and Solda Ironstone. Illite has been used as thermal indicator for the past thermal activity, grade of metamorphism, and rock-water interactions during the diagenesis or the maturation of the basin. Clay minerals are usually crystalline throughout the reactions, occur during basin diagenesis accompanied by the loss of water which leads to mobilize variable amount of cations (e.g. Ca, Na, K and Si) from the clay structures. Hexavalent form of uranium (U^{6+}) is readily soluble in oxidizing conditions. The dissolved uranium is absorbed by an ion-exchange mechanism in clay minerals (Davey and Scott, 1956). The Sonrai basin being structurally (faulting, fracturing, folding, and unconfomities) controlled having potential to host uranium mineralization. Mineralization is confined to the Gorakalan graphitic shales, Rohini carbonates, Bandai sandstone and shales of the Sonrai Formation due to Kurrat volcanic (hydrothermal) activity that provided time and space (reducing conditions) for the precipitation of uranium in and along the fractures or weak-zones. These rock units are pyrite bearing clay-organic rich facies where the pre-existing clays (kaolinite and smectite) have been hydrothermally altered into chlorite and illite (tv-1M polytype) in the vicinity of weak-zones. Illitization/ chloritization is the characteristic feature of the unconformity-related Proterozoic uranium mineralization in the world. It is concluded that the Illite-chlorite-Mg-smectite

clay mineral assemblage is associated with uranium mineralization and kaolinite-chlorite-Na-smectite is related to barren rocks. These deposits are found almost entirely in reducing conditions. The organic carbon is considered as one of the most possible reductant to remove uranium from the solution as carbonate from ore zones contains some organic carbon (Brookins, 1981). Uranium ions most likely carried in the solution in oxidation state as oxy-ions, although possibility of transport of these ions as organic complexes cannot be ruled out. Remobilization and re-precipitation of these ions under the redox conditions redistribute ore at the time of their formation. Present study on clay mineral assemblages / clay-types, palaeoclimatic conditions and clay-crystallinities demonstrate occurrence of uranium mineralization in the Sonrai Formation as well as possibility of migrated uranium concentration along the unconformities of the Sonrai basin.

Acknowledgements: JPS and SKJ (JRF) acknowledge Ministry of Earth Sciences, Government of India for financial support towards this work in the form of a Project Grant (MoES/Hydro-Sulphides/04/08-PC-II).

References

Ahn, J.H., Peacor, D.R. and Coombs, D.S. (1988) Formation mechanisms of illite, chlorite and mixed–layer illite chlorite in Triassic volcanogenic sediments from the Southland Syncline, New Zealand. Contrib. Mineral. Petrol., v.99, pp.82-89.

Alexander, L. and Klug, H.P. (1948) Basic aspects of x–ray absorption in quantitative diffraction analysis of powder mixtures. Anal. Chem., v.20, pp.886-889.

Alt, J. (1999) Very low–grade hydrothermal metamorphism of basic igneous rocks in Low–grade metamorphism. *In:* M. Frey and D. Robinson (Eds.). Blackwell, Oxford, pp.169-201.

Beaufort, D., Meunier, A., Patrier, P. and Ottaviani, M.M. (1992) Significance of the chemical variations in assemblages including epidote and or chlorite in the fossil geothermal field of Saint Martin (Lesser Antilles). Jour. Volcan. Geotherm. Res., v.51, pp.95-114.

Beaufort, D., Patrier, P. and Laverret, E. (2005) Clay alteration associated with Proterozoic unconformity–type uranium deposits in the East Alligator Rivers uranium field, Northern Territory, Australia. Econ. Geol., v.100(3), pp.515-536.

Berger, I.A. (1974) The role of organic matter in the accumulation of uranium: The organic geochemistry of coal–uranium association. Proc. Series (IAEA, IAEA–SM 183/29), pp.99-123.

Biscay, P.E. (1965) Mineralogy and sedimentation of recent deep sea clay in the Atlantic Ocean and adjacent seas and oceans. Geol. Soc. Amer. Bull., v.76, pp.803-832.

Blatt, H., Middleton, G.V. and Murray, R.C. (1980) Origin of Sedimentary Rocks. Englewood Cliffs, N.J., Prentice Hall, 782p.

Boles, J.E. and Franks, S.G. (1979) Clay diagenesis in Wilcox sandstones of southwest Texas: implications of smectite diagenesis on sandstone cementation. Jour. Sediment. Petrol., v.49, pp.55-70.

Borovec, Z. (1981) The Adsorption of Uranyl Species by Fine Clay. Chem. Geol., v.32, pp.45-58.

Brime, C. (1981) Post depositional transformation of clays in Palaeozoic rocks of northwest Spain. Clays and Clay Mineral., p.16.

Brookins, D.G. (1981) Geochemistry of clay minerals for uranium exploration in the Grants mineral belt, New Mexico. Miner. Diposit, v.17 (1), pp.1432-1866.

Brown, G. (1961) The X–ray identification and crystal structure of clay minerals. Miner. Soc. London, 544p.

Davey, P.T. and Scott, T.R. (1956) Adsorption of uranium on clay minerals. Nature, v.178, 1195p.

Drever, J.J. (1973) The preparation of oriented clay mineral specimens for X–ray diffraction of analysis by a filter membrane peel technique. Amer. Mineral., v.58, pp.553-554.

Drief, A. and Nieto, F. (2000) Chemical composition of smectites formed in clastic sediments: Implications for the smectite–illite transformation. Clay Mineral., v.35, pp.665-678.

Dunoyer de Segongac, G. (1970) The transformation of clay minerals during diagenesis and lowgrade metamorphism. Sedimentology, v.15, pp.281-348.

Eberl, D.D. and Srodon, J. (1988) Ostwald ripening and interparticle–diffraction effects for illite crystals. Amer. Miner., v.73, pp.1335-1345.

Ehrenberg, S.N., Aagaard, P., Wilson, M.J., Fraser, A.R. and Duthie, D.M.L. (1993) Depth–dependent transformation of kaolinite to dickite in sandstones of the Norwegian continental shelf. Clay Mineral., v.28, pp.325-352.

Essene, E.J. and Peacor, D.R. (1995) Clay mineral thermometry a critical perspective. Clays and Clay Mineral., v.43, pp.540-553.

Frey, M. and Robinson, D. (1999) Low-Grade Metamorphism. London, Blackwell Science, pp.29-31.

Grim, R.E., Bradley W.F. and Brown, G. (1951) X-ray identification and crystal structures of clay minerals. *In:* G.W. Brindley (Ed). Mineral. Soc. London, pp.138-172.

Guggenheim, S., Bain, D., Bergaya, F., Brigatti, M.F., Drits, V.A., Eberl, D.D., Formoso, M.L.L., Galan, E., Merriman, R.J., Peacor, D.R., Stanjek, H. and Watanabe T. (2002) Report of the Association Internationale pour l'Etude des Argiles (AIPEA) Nomenclature Committee for 2001: Order, disorder and crystallinity in phyllosilicates and the use of the "crystallinity index". Clay Minerals, v.37, pp.389-393.

Harper, D.A., Longstaffe, F.J., Wadleigh, M.A. and McNutt,

R.H. (1995) Secondary K–feldspar at the Precambrian–Paleozoic unconformity, southwestern Ontario. Can. Jour. Earth Sci., v.32, pp.1432-1450.

Hashimoto, Y., Tadai, O., Tanimizu, M., Tanikawa, W., Hirono, T., Lin, W., Mishima, T., Sakaguchi, M., Soh W., Song, S.R., Aoike, K., Ishikawa, T., Murayama, M., Fujimoto, K., Fukuchi, T., Ikehara, M., Ito, H., Kikuta, H., Kinoshita, M., Masuda, K., Matsubara, T., Matsubayashi, O., Mizoguchi, K., Nakamura, N., Otsuki, K., Shimamoto, T., Sone, H. and Takahashi, M., (2008) Characteristics of chlorites in seismogenic fault zones: the Taiwan Chelungpu fault drilling project (TCDP) core sample. Earth, v.3, 16p.

Hoeve, J. and Quirt, D. (1987) A stationary redox front as a critical factor in the formation of high grade unconformity-type uranium ores in the Athabasca basin, Saskatchewan, Canada. Bull. Deposit. Mineral., v.110, pp.157-171.

Hooton, D.H. and Giorgetta, N.E. (1977) Quantitative x–ray diffraction analysis by a direct calculation method. X–ray Spect., v.6(1), pp.2-5.

Hower, J., Eslinger, E.V., Hower, M.E. and Perry, E.A. (1976) Mechanism of burial metamorphism of argillaceous sediments: Mineralogical and chemical evidence. Geol. Soc. Amer. Bull., v.87, pp.725-737.

Iida, Y. (1993) Alteration and ore–forming processes of unconformity related uranium deposits. Resour. Geol., v.15, pp.299-308.

Iman, M.B. and Shaw, E.H.F. (1985) The diagenesis of Neogene clastic sediments from the Bengal basins Bangladesh. Jour. Sediment. Petrol., v.55, pp.665-671.

Izquierdo, G., Cathelmeau, M. and Alfonsom, (1995) Clay minerals, fluid inclusions and stabilized temperature estimation in two wells from Los Azufres geothermal field, Mexico. Proceedings of the world geothermal congress, Florence, Italy. Internat. Geothermal Assoc., pp.1083-1086.

Jackson, M.L. (1969) Soil chemical analysis advanced course, 5th print. Department of Soil Science University, Wisconsin, Madison WI, 894p.

Jones, B.F. and Galan, E. (1988) Sepiolite and palygorskite: Hydrous phyllosilicates (Exclusive of micas). *In:* S.W. Bailey (Ed). Reviews in Mineralogy 19, Mineral. Soc. Amer., pp.631-674.

Keil, R.G., Monflugon, D.B., Prahl, F.G. and Hedges, J.I. (1994) Sorptive preservation of labile organic matter in marine sediments. Nature, v.370, pp.549-552.

Kisch, H.J. (1983) Mineralogy and petrology of burial diagenesis (burial metamorphism) and incipient metamorphism in clastic rocks. *In:* Rocks G. Larsen and G.V. Chilingar, (Eds.), Diagenesis of Sediments and Sedimentary Elsevier, Amsterdam. pp.289-493.

Kubler, B. (1984) Les indicateurs des transformations physiques et chimiques dans la diagenese, temprature et calorimetrie. *In:* M. Lagache, (Ed.), Thermometrie et Barometrie Geologiques. Societe Francaise Mineralogie et de Cristallographie, pp.489-596.

Laird, D.A. (2006) Influence of layer charge on swelling of smectites, Appl. Clay Sci. v.34, pp.74-87.

Lanson, B., Beaufort, D., Berger, G., Bauer, A., Cassagnabere, A. and Meunier, A. (2002) Authigenic kaolin and illitic minerals during burial diagenesis of sandstones: A review. Clay Minerals, v.37, pp.1-22.

Laverret E., Mas, P.P., Beaufort, D., Kister, P., Quirt, D., Bruneton, P. and Clauer, N. (2006) Mineralogy and geochemistry of the host-rock alterations associated with the Shea Creek unconformity-type uranium deposits. Athabasca basin, Saskatchewan, Canada. Part-1. spatial variation of illite properties. Clays and Clay Mineral., v.54(3), pp.275-294.

Madejova, J. (2003) FTIR techniques in clay mineral studies, Vib. Spectrosc., v.31, pp.1–10.

Mahadevan, T.M. (1986) Space-time controls in Precambrian uranium mineralisation in India. Jour. Geol. Soc. India, v.27, pp.47-62.

Merriman, R.J. and Peacor, D.R. (1999) Very low grade metapelites: Mineralogy, microfabrics and measuring reaction progress. *In:* M. Frey and D. Robinson (Eds.), Low–Grade Metamorphism. Blackwell Science Ltd., Oxford, pp.10-60.

Mishra, B. (1996) Annual report on the exploratory drilling at Sonrai, Lalitpur District., U.P., AMD.

Morse, J.W. and Casey, J.C. (1988) Ostwald processes and mineral paragenesis in sediments. Amer. Jour. Sci., v.288, pp.537-560.

Pacquet, A. and Weber, F. (1993) Petrographie et mineralogie des halos d'alteration autour du gisement de Cigare Lake et leurs relations avec les mineralisations. Can. Jour. Earth Sci., v.30, pp.674-688.

Patrier, P., Beaufort, D., Laverret, E. and Bruneton, P. (2003) High-grade diagenetic $2M_1$ illite from the Middle Proterozoic Kombolgie Formation (Northern Territory, Australia). Clays Clay Minerals., v.51, pp.102-116.

Peacor, D.R. (1992) Diagenesis and low–grade metamorphism of shales and slates. Minerals and Reactions at the Atomic Scale: Transmission Electron Microscopy. *In:* P.R. Buseck (Eds.). Reviews in Mineralogy. Mineral. Soc. Amer., v.27, pp.335-380.

Percival, J.B. and Kodama, H. (1989) Sudoite from Cigar Lake, Saskatchewan. Can. Mineral., v.27, pp.633-641.

Pollastro, R.M. (1982) A recommended procedure for the preparation of oriented clay–mineral specimens for X–ray diffraction analysis: Modifications to Drever's filter–membrane peel technique. USGS Open File Report, pp.82-71.

Poppe, L.J., Paskevich, V.F., Hathaway, J.C. and Blackwood, D.S. (2002) A laboratory manual for X-ray powder diffraction. USGS Open File Report, pp.1-41.

Prakash, R., Swarup, P. and Srivastava, R.N. (1975) Geology and mineralization in the southern parts of Bundelkhand in Lalitpur dist., U.P. Jour. Geol. Soc. India, v.16, pp.143–156.

Ramaekers, P., Jefferson, C.W., Yeo, G.M., Collier, B., Long, D.G.F., Catuneanu, O., Bernier, S., Kupsch, B., Post, R., Drever, G., McHardy, S., Jiricka, D., Cutts, C. and Wheatley, K. (2005a) Revised geological map and stratigraphy of the Athabasca Group, Saskatchewan and Alberta.

RAMAEKERS, P., YEO, G.M., JEFFERSON, C.W., COLLIER, B., LONG, D.G.F., CATUNEANU, O., BERNIER, S., KUPSCH, B., POST, R., DREVER, G., MCHARDY, S., JIRICKA, D., CUTTS, C. and WHEATLEY, K. (2005b) Revised geological map and stratigraphy of the Athabasca Group, Saskatchewan and Alberta. *In:* C.W. Jefferson and G. Delaney, (Eds.), Geology and Uranium Exploration Technology of the Proterozoic Athabasca Basin, Saskatchewan and Alberta. Geol. Surv. Canada, Bull., v.588.

RETALLACK, G.J. (1986a) The fossil record of soils. *In:* V.P. Wright (Ed.), Paleosols: Their recognition and interpretation. Oxford, Blackwells, 315p.

ROY, M., BAGCHI, A.K., BABU, E.V.S.S.K., MISHRA, B. and KRISHNAMURITHY, P. (2004) Petromineragraphy and mineral chemistry of bituminous shale-hosted uranium mineralization at Sonrai, Lalitpur district, Uttar Prdaesh. Jour. Geol. Soc. India, v.63, pp.291-298.

ROY, M., ROY, A.K. and PARIHAR, P.S. (2008) Radioactive carbonaceous material within the fractured Bundelkhand granite of Gwalior Basin at Dursendi, Gwalior district. Madhya Pradesh – A petrographic revelation. Jour. Geol. Soc. India, v.72, pp.479-483.

RUIZ CRUZ, M.D. and ANDREO, B. (1996) Genesis and transformation of dickite in Permo-Triassic sediments (Betic Cordilleras, Spain). Clay Mineral., v.31, pp.133-52.

SHARMA, K.K. (2000) Evolution of the Archaean–Palaeoproterozoic crust of the Bundelkhand Craton, Northern Indian Shield. *In*: O.P. Verma and T.M. Mahadevan (Eds.), Research Highlights in Earth Sciences, DST, India. Geol. Cong., v.1, pp.95–105.

SINGH, J. and BAGCHI, A.K. (1994) Possibility of occurrence of breccia complex–cum–Iron oxide type uranium deposit at the contact of the Solda and Sonrai Formations of Bijawar Group in Lalitpur Dist., U.P. Extended Abst. On First order Uranium exploration Target selection in the Proterozoic Solda India, AMD, pp.5-6.

SINGH, K.K. and GOYAL, R.S. (1972) Copper mineralisation in the Bijawar series around Sonrai, District Jhansi, U.P. Jour. Geol. Soc. India, v.13(4), pp.252-360.

SOPUCK, V.J., DE CARLE, E.M. and COOPER, B. (1983) The application of lithogeochemistry in the search for unconformity-type uranium deposits, northern Saskatchewan, Canada, *In:* G.R. Parslow (Eds.), Jour. Geochem. Explor., v.19, pp.77-99.

SRIVASTAVA, R.N. (1989) Bijawar phospherites at Sonrai geology, sedimentation, exploration strategy and origin. Mem. Geol. Soc. India, v.13, pp.47-59.

SRODON, J. (1984) X–ray powder diffraction identification of illitic materials: Clays and Clay Miner., v.32, p.337-349.

TAN, K.H. (2005) Soil sampling, preparation, and analysis. (2nd ed.). CRC press, Taylor & Francis Group. 623p.

TUCKER, M. (Ed.) (1988) Techniques in Sedimentology. Blackwell Science Inc, 408p.

UPADHYAYA, T.P., RAJU, S. and SINGH, D.P. (1990) Second generation mapping of Bundelkhand granites and Bijawar group of rocks in parts of Lalitpur district, U.P., Geol. Surv. India records, v.126, pp.44-48.

VAN DE KAMP, P.C. (2008) Smectite-illite-muscovite transformations, quartz dissolution, and silica release in shales. Clays and Clay Miner., v.56(1), pp.66-81.

VELDE, B. (1985) Clay Minerals: A Physico–Chemical Explanation of their Occurrence. Elsevier, Amsterdam, 427p.

WEAVER, C.E. (1958b) Geological interpretation of argillaceous sedimentary rocks. Bull. Amer. Assoc. Petrol. Geol., v.42, pp.254-271.

WEAVER, C.E. (1958c) A discussion of the origin of clay minerals in sedimentary rocks. Clays Clay Mineral., v.5, pp.159-173.

WILSON, M.J. (1987) A handbook of determinative methods in clay mineralogy. *In:* M.J. Wilson (Ed). Blackie-Son Ltd., London, 308 p.

YANG, Y.L. and APLIN, A.C. (1997) A method for the disaggregation of mudstones. Sedimentology, v.44, pp.559-562.

ZIEGLER, K. and LONGSTAFFE, F.J. (2000) Multiple episodes of clay alteration at the Precambrian/Paleozoic unconformity, Appalachian Basin: Isotopic evidence for long–distance and local fluid migrations. Clays and Clay Mineral., v.48(4), pp.474-493.

(Received: 21 August 2010; Revised form accepted: 20 July 2011)